Iran. J. Radiat. Res., 2007; 5 (1): 23-30

A comparative Monte Carlo study on 6MV photon beam characteristics of Varian 21EX and Elekta SL-25 linacs

A. Mesbahi*, P. Mehnati, A. Keshtkar

Department of Medical Physics, Medical School, Tabriz University of Medical Sciences, Tabriz, Iran

Background: Monte Carlo method (MC) has played an important role in design and optimization of medical linacs head and beam modeling. The purpose of this study was to compare photon beam features of two commercial linacs, Varian 21EX and Elekta SL-25 using MCNP4C MC code. ***Materials and Methods:*** The 6MV photon beams of Varian 21EX and Elekta SL-25 linacs were simulated based on manufacturers provided information. Photon energy spectra and absolute absorbed dose values were calculated for field sizes of 10×10 and 20×20 cm^2. Also, contamination electron spectra for field size of 20 ×20 cm^2 were scored for both linacs. ***Results:*** Our results showed that the relative absorbed dose values and contamination electron spectrum were similar and comparable, but photon fluence and absolute absorbed dose values were 17% and 13% higher for Varian linac respectively for the field size of 10×10 cm^2. ***Conclusion:*** Despite the differences in head components of two commercial linacs, their relative depth dose values were very close to each other. The absolute dose per incident electron showed some discrepancy, as well. Thus, this study suggests the use of absolute absorbed dose values as an invaluable factor when different linacs head are compared using Monte Carlo Method. **Iran. J. Radiat. Res., 2007; 5 (1): 23-30**

Keywords: *Dosimetric features, Elekta SL-25, Varian 21EX, Monte Carlo method.*

INTRODUCTION

The application of the Monte Carlo (MC) method in radiation therapy was first postulated by Mackie and Battista [1], since that time MC method has been used in many areas including radiation dosimetry, treatment machines, and treatment planning calculations [2-10]. MC method is a powerful tool for the study of the effect of Linac head components on dosimetric characteristics of photon and electron beams [4]. Different medical linacs are available in the market and their beam characteristics including percent depth doses (PDDs), and dose profiles are close to each other for a given energy of primary electron beam. But, some characteristics such as photon and electron spectra and build up dose may be different [3]. These differences are mainly originate from the different geometry and materials used in X-ray target and flattening filter (FF) and other components placed in the pathway of photons coming from target [4]. However, it is very difficult to calculate and measure the electron and photon energy spectra of clinical linear accelerators. On the other hand, accurate calculation of bremstrahlung spectra is a prerequisite to many other MC calculations in medical radiation dosimetry, such as MC-based treatment planning. More complex analytical methods have been applied but the MC method has been used as a powerful and the most comprehensive method to generate photon and electron spectra of clinical linacs [3, 11, 12].

Several studies have been done on electron contamination sources for clinical photon beams [13-15] showing that the dominant sources of electron contamination were the FF and the beam monitor chamber. Some earlier and recent experimental studies have developed methods to reduce electron contamination and thus the surface dose. MC simulation of contamination electron spectra for different photon beams have been studied for accuracy of MC-based treatment planning

*Corresponding author:
Dr. Asghar Mesbahi, Department of Medical Physics, Medical School, Tabriz University of Medical Sciences, Tabriz, Iran.
Fax: *+98 411 3364660*
E-mail: *asgharmesbahi@yahoo.com*

calculations [16].

On the other hand issue is that the absolute absorbed dose per incident electron on target for different linacs have not been studied completely yet. This factor indicating the dose rate per initial electron, may affect the treatment time, and electron gun and magnetron or klystron lifespan as well. In a study Sheikh-Bagheri and Rogers. (2002), have shown that Siemens linac produces more photons per incident electron than Varian and Elekta linacs on phantom surface. They attributed this discrepancy to differences in incident electron energies and ignored the differences in electron beam diameter and different composition of target and FF [2, 3].

In the current research, two commercial medical linacs were simulated using MCNP4C MC code, and their dosimetric characteristics were calculated and compared. Also, the impact of different material composition and geometry of target and FF of both linacs on electron and photon energy spectra and depth dose values were evaluated.

MATERIALS AND METHODS

MC modeling of linacs

Two 6MV photons beam models for Varian 2100EX (Varian Medical Systems, Palo Alto, CA, USA) and Elekta SL-25 (Elekta oncology systems, Stockholm, Sweden) using version 4C of the MCNP radiation transport code [17]. A schematic representation of the linacs heads and their components are shown in figure 1. The head components, including the target, primary collimator, FF, and secondary collimator jaws, were simulated based on manufacturer-provided information. The target was composed of tungsten and copper layers with different thicknesses for both linacs. The FF of Varian linac was made from copper with density of 8.93 g/cm^3 and atomic number of 29; yet, for Elekta it was made of stainless steel with density of 7.9 g/cm^3 and atomic number of 26.

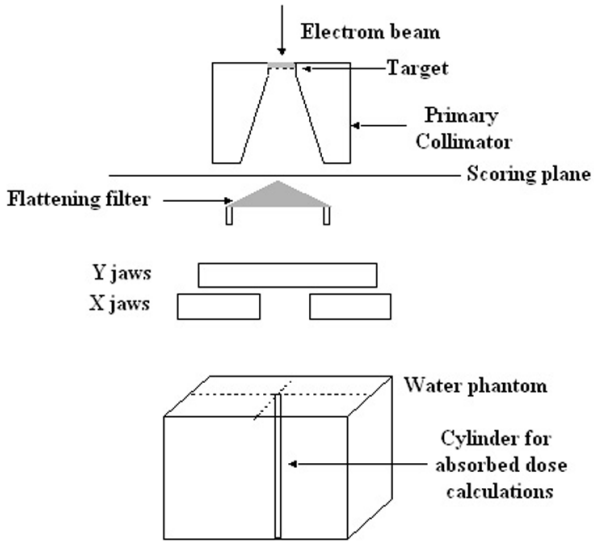

Figure 1. The schematic representation of simulated geometry including both linacs head, the position of scoring plane for phase space file generation and water phantom.

A water phantom with dimensions of 50 × 50 × 50 cm^3 was simulated under treatment head to score absolute and relative absorbed doses. A mono-energetic electron beam with uniform spatial distribution and 2 mm diameter was simulated [6, 7].

The dose calculation process was done in two distinct steps. First, an initial MC simulation of the accelerator head was performed to produce the phase space (PS) file. Second, by running PS file from scoring plane the absorbed doses were calculated in water phantom. For PS file generation, a scoring plane was defined above the FF and under target. Then, we commissioned our beam model through comparing the calculated percentage depth doses and beam profiles with the measured data. The PDDs and beam profiles for 5×5 cm^2, 10×10 cm^2, and 30×30 cm^2 field sizes were calculated and compared with the measured data. The beam profiles were calculated at depth of 10 cm. For each point, the local difference relative to the measured dose at that point was calculated and used for model validation.

For dose calculations in the water phantom, PS files were generated using 30×10^6 initial electron and 18×10^6 particle crossed the scoring plane and their history recorded in PS file. Photon and electron energy cut-offs of 10 and 500 keV were used.

For a PS file generation, the run-time was about 1500 minutes, and for dose calculations in water phantom the run-time decreased to 120 minutes with a 3 GHz personal computer.

For dose calculation in water phantom, a cylinder with radius equal to one-tenth of the beam diameter along the central axis of the beam was considered, and divided into scoring cells with a height of 2 mm. By running particles in PS file through the water phantom, the energy deposited in each scoring cell was calculated by *F8 tally. The same approach was used for the beam profile, except that of the central axis of the scoring cylinder which was vertical to the central axis of the beam, and the cylinder was at the depth of 10 cm. The diameter of the cylinders was 4 mm and divided into cells with 2 mm thickness along the central axis. Resolution for beam profiles was 2 mm laterally. Statistical uncertainty of MC results was less than 1.5% for PDD and beam profile calculations. One way to increase the number of photons crossing the phase space plane per initial electron and reducing the run time has been increase in the number of bremsstrahlung photons generated per incident electron on target. This would be possible by changing the BNUM default value in PHYS card for electrons in the MCNP input file [17]. The optimum number was set to 80 according to our previous work [7]. Dose measurements were carried out by Scanditronix automatic water phantom (RFA-300, Scanditronix Wellhofer AB, Sweden) and an ionization chamber (RK, Scanditronix Wellhofer AB, Sweden) with 0.12 cm^3 volume. Measured results corrected for measurement point displacement of 1mm toward the phantom surface.

Electron beam energy tuning was performed by comparing calculated and measured PDD curves for 10×10 cm^2 field size. To compare calculation and measurements, the value of each cell was normalized to the maximum value of energy deposited in the central axis. For a 6 MV photon beam, the energies of 6.0, 6.2, 6.3, 6.4, and 6.5 MeV were used. For primary electron energy determination, the results of measurements and calculations were compared and the best match determined the optimum energy of the electron beam. Local differences between simulation and measurement results were calculated for accurate comparison between results.

After MC model's validations, some dosimetric features of both linacs were compared. To find out the effect of different composition of target and FF on photon and electron energy spectra, and absolute absorbed dose values, it was required to have the same energy and beam width for incident electron beam for both linacs. It has been shown that the electron beam diameter and energy affects the amount of absorbed dose per initial electron [7].

Photon energy spectra were calculated using F5 tally, using a virtual ring detector to tally the number of photons crossing the detector ring. The diameter of detector ring was equal to field size on the phantom surface. For electron energy spectra, a void cell with thickness of 0.001 mm and 20×20 cm^2 was considered at phantom surface, and the electrons crossing the cell was scored using f4 tally. The field size for electron energy spectra calculation was 20×20 cm^2.

RESULTS AND DISCUSSION

MC modeling of linacs

The primary electron energies of 6.1 and 6.4 MeV were selected for Varian and Elekta respectively. MC calculated PDDs and beam profiles were compared with measurement to validate our MC models. There was good agreement between measurement and calculation for PDDs and beam profiles (figures 2-4). For PDDs, discrepancy between calculations and measurements in descending part was less than 2% and it increased up to 15% in build up region. For beam profiles, differences less than 2% were seen for flat region for both linacs, but it increased to 10% for region located out of field (figure 4). The same results have also

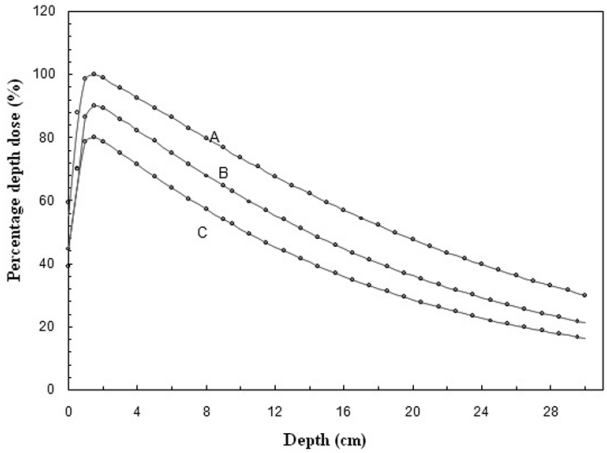

Figure 2. Percent depth dose curves of 6 MV beam of Elekta linac for different field sizes (A) 30×30 cm² (B) 10×10 cm² (C) 5×5 cm². The curves B and C were scaled to 0.9 and 0.8 to inclusion on the same graph.

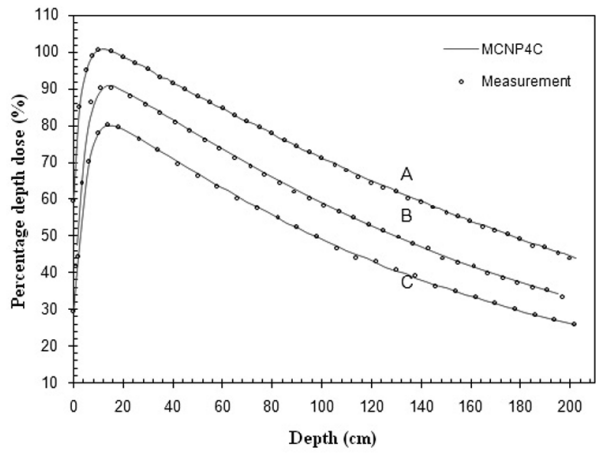

Figure 3. Percent depth dose curves of 6 MV beam of Varian linac for different field sizes (A) 30 ×30 cm² (B) 10×10 cm² (C) 5×5 cm². The curves B and C were scaled to 0.9 and 0.8 to inclusion on the same graph.

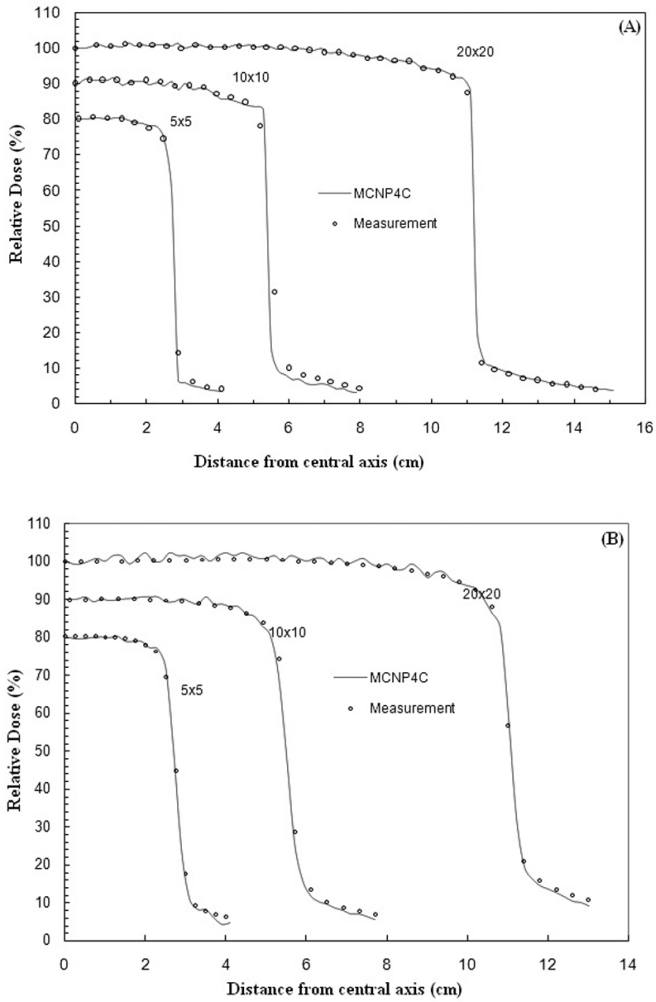

Figure 4. Beam profiles at the depth of 10 cm for (A) Elekta (B) Varian linacs for different field sizes.

been reported in previous studies [2-9].

Photon energy spectra

The photon energy spectra of both linacs at 8 cm from target (above FF) and also phantom surface were calculated (figure 5). The photon energy spectra after target was calculated using ring detector tally with radius of 1cm. Comparing the photon spectra above FF shows that the total calculated bremsstrahlung yield (integrated over energy) is 40% higher for Varian linac and it is predictable due to thinner target layers (Tungsten plus Copper) for Varian relative to Elekta. The self-absorption increased with target thickness especially for low energy photons and caused some degree of spectra hardening for photon beams. Also, one should keep in mind that total bremsstrahlung yield was not calculated and compared in our simulation and only the photons with direction angle of less than 7 degree relative to central axis of beam were scored in our simulation only. However, the comparison of bremsstrahlung yield integrated over all angles could present different results [12, 18].

Photon energy spectra at phantom surface were calculated using ring detectors with 5 cm and 10 cm radius for field sizes of 10×10 and 20×20 cm²,

respectively (figure 6). As seen, the photon fluence of Varian is higher than Elekta for whole energy range from 0 to 6 MeV photons. The photon fluence integrated over energy is 17% and 14% higher for Varian relative to Elekta for field sizes of 10×10 and 20×20 cm², respectively. Similar results were reported by Sheikh-Bagheri and Rogers (2002) [3]. In their study, 10% higher photon fluence was seen for 6MV photon beam of Varian relative to Elekta. Of course, it should be reminded that their scoring ring radius and MC code was different from the current study.

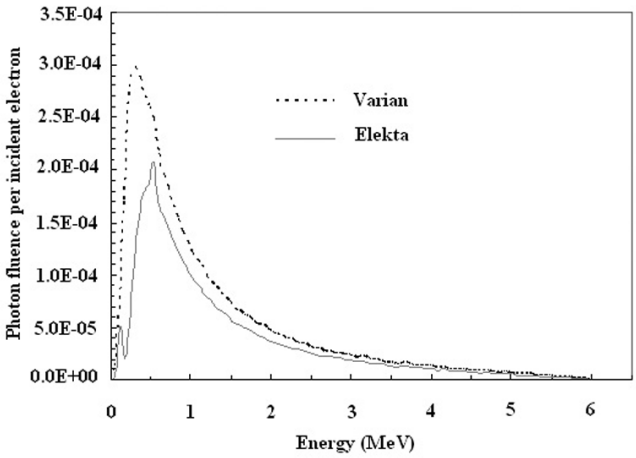

Figure 5. Photon energy spectra of Elekta and Varian linacs at a distance of 8 cm from target using 1cm radius ring detector.

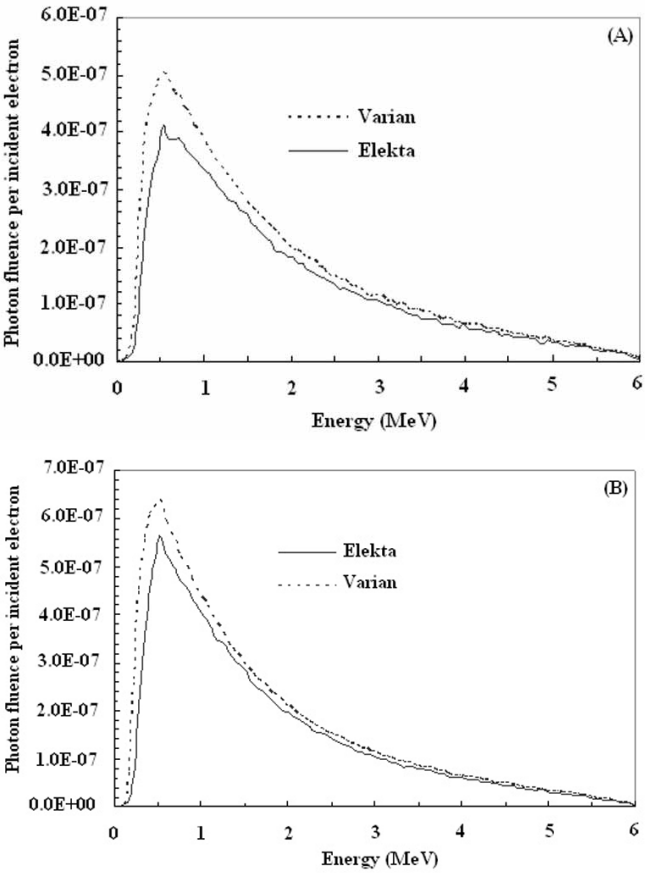

Figure 6. Photon energy spectra for 6MV photon beams of Varian and Elekta linacs for different field sizes. (A) 10×10 cm² (B) 20×20 cm².

To characterize the quality of a particular photon beam from a medical linear accelerator, the energy spectrum is the ultimate descriptive function; because, the dosimetric properties of the radiation beam are directly tied to this function. A clinical photon beam mainly consists of three components; i.e., primary photons, scattered photons and contaminant electrons. Primary photons come directly from the target to the patient. Scattered photons are generated or scattered in the accelerator components other than the target mainly FF. Recent studies on FF have showed that it's removing can increase dose rate almost by a factor of 2 for 6 MV photon beams. Also, the dose rate increase differs by energy of photon beam for different medical linacs [19-21]. In a study on 6MV photon beam of Varian 2100EX, the dose rate increase of 2.31 was observed for field size of 10×10 cm² [19]. In another study on 6MV photon beam of Elekta SL-25 a dose rate increase of 2.35 was reported for the same field size [21]. To compare the two linacs show that the FF of both linacs acts very similarly and their differences in FF material results in only 5% difference in scattering and absorption of primary photons coming from target [19-21]. Thus, it could be concluded that the observed discrepancy in total photon fluence on phantom surface originates from different thickness of tungsten and copper layers in both linacs.

Contamination electron spectra on phantom surface

We calculated contamination electron energy spectrum for both linacs using F4 tally on phantom surface for field size of 20×20 cm² (figure 7). It is seen that the electron energy spectra for both linacs have similar pattern with photon energy spectra.

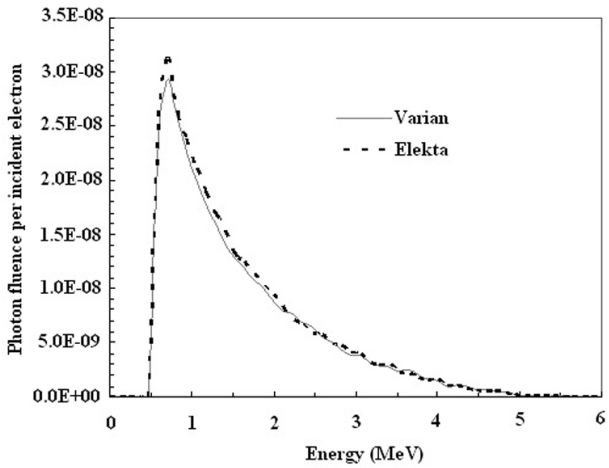

Figure 7. Contamination electron energy spectra for Elekta and Varian linacs on phantom surface for field size of 20×20 cm².

Comparing the absolute electron fluence per incident electron for whole energy range showed 4% higher fluence for Elekta linac. But, there was seen relatively good agreement between photon fluences for both linac in whole energy range. It seemed that the difference is not too large to be conclusive according to our statistical uncertainty of 2% for electron spectra calculations. However, studies on electron contamination sources in linacs have showed that for wide opening of the collimators, the main sources are the FF and the air below it [14]. If we exclude the effect of air below FF because of equal thickness of air column for both linacs, this difference could arise from different material and thickness of FF used in both linacs. The FF of Varian linac was made of copper with density of 8.93 g/cm³ and atomic number of 29. But, for Elekta it was made of stainless steel with density of 7.9 g/cm³ and atomic number of 26. So, it seems that the effect of atomic number is negligible due to dominant role of Compton effect in photon interactions with FF in energy range used in our study. The FF absorbs the secondary electrons generated in the target, primary collimator and the air inside the head. The secondary electrons generated by the FF produced a wide energy spectrum with mean energies of the same order of the bremsstrahlung spectrum.

The knowledge of the electron contamination characteristics is important in clinical dosimetry [15]. Contaminant electrons contribute only to the surface dose distribution and the dose at shadow depths. In a study by Butson *et al.* (2000) MC simulations using MCNP4A and experimental work have been performed to evaluate the contribution of electrons which are produced in air from a 6 MV photon beam. Results showed that up to 9% of applied dose was delivered to a patient's skin surface from electrons excited in the irradiated air column [13]. In another study Ding (2002) investigated the surface doses contributed by charged particles of 6 and 18 MV photon beams for Varian 21EX accelerator. The results showed that at 6 MV, the maximum charged particle contamination doses at the surface were 7% for a 10 × 10 cm² field and 21% for a 40 × 40 cm² field. At 18 MV, the doses were up to 11% for a 10 × 10 cm² field and 29% for a 40 × 40 cm² field. This study suggested that the accurate beam modeling for dosimetry and treatment planning purposes must take electron contamination into account [22].

Comparison of depth dose curves of both linacs

In order to remove the effect of different initial electron energy on depth dose values, we calculated the absolute depth dose values of both linacs with initial electron energy of 6 MeV. The PDD and absolute depth dose values are shown in figures 8 and 9. It is evident that the dose per initial electron is higher for Varian and it is 13% and 9% higher than Elekta for field sizes of 10×10 and 20×20 cm² respectively. So, the number of photons hitting the water phantom per incident electron is higher for Varian linac which was described previously. The target of Elekta linac is thicker that Varian linac which cause more primary photon absorption. It may be a superiority of Varian linac to Elekta, because in order to create the same dose rate for 10×10 cm² field size, the Elekta linac will need about 13% more electrons, which increase, the workload of electron generating and accelerating components. Therefore, it

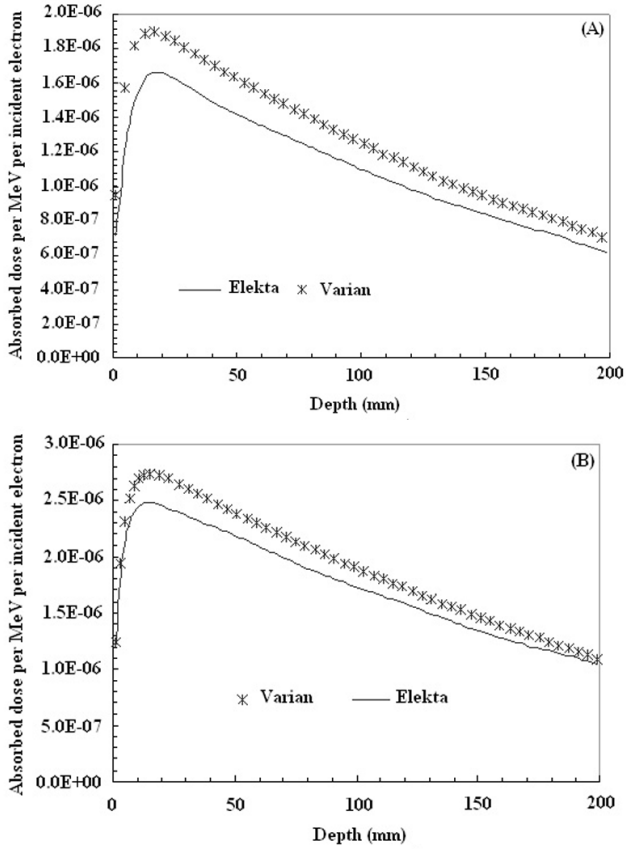

Figure 8. Absorbed dose per MeV per incident electron for 6MV photon beams of Varian and Elekta linacs. (A) 10×10 cm² (B) 20×20 cm².

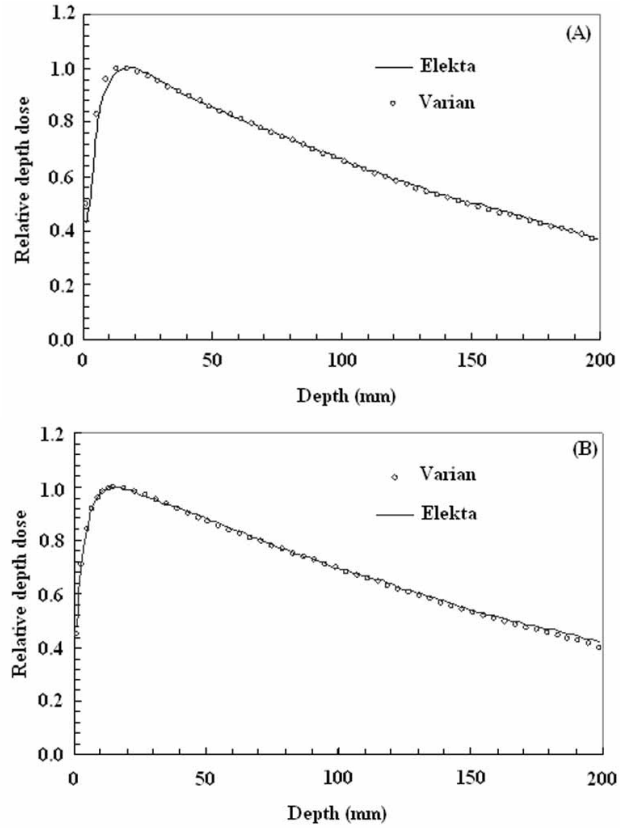

Figure 9. Relative depth dose curves for 6MV photon beams of Elekta and Varian linacs. (A) 10×10 cm² (B) 20×20 cm² field sizes.

may have some applications for MLC-based treatments which need more time and photon fluence in comparison with conventional treatments.

Comparing PDD curves showed that relative depth dose values were very close together and their differences were less than 2% for all depths. Also, there was good agreement between two PDD curves in build up region and maximum difference was observed for 20×20cm² field sizes, and it was less than 5% which can be explained according to our obtained results on photon and contamination spectra in the previous section. It is known that two main contributions to the dose at the phantom surface and build up region are electrons generated by primary and secondary photon interactions within the water and electrons coming from linac head. As it was discussed the photon energy spectra of both linacs had very similar patterns and if they were normalized to maximum value in the spectrum, they would have overlapped each other. On the other hand, contamination electron spectra on phantom surface were in close agreement, and their fluence difference was less than 4%. This little difference could have caused a negligible discrepancy between PDD curves of linacs. Our results were consistent with results of Paelinck *et al.* in which they reported that despite the differences measured in build-up dose for single beams between the Elekta and the Varian linear accelerator, there were no measurable differences in superficial dose when a typical IMRT dose plan of 6 MV for a head and neck tumor is executed at the two machines [23].

CONCLUSION

The results showed the higher photon fluence for Varian linac. The contamination

electron energy spectra showed similar pattern and fluence for both linacs. Absolute and relative absorbed dose curves in water phantom were compared. Excellent match between PDD curves and in build up region were observed for different field sizes. But, the absolute absorbed dose values were higher for Varian in comparison with Elekta due to greater photon fluence for Varian linac. Although the PDD curves of both linacs are similar for 6MV photon beam, some dosimetric features including the absolute absorbed dose (dose rate) can be different because of differences in thickness of target materials. The results of this study suggested that the calculation of absolute absorbed dose in MC simulation of clinical linacs could provide useful information about the effect of materials and geometries used in linac head components.

ACKNOWLEDGMENT

A part of this study was supported financially by research office of Tabriz University of Medical Sciences. We would like to thank Dr. Farajollahi for his assistance with this project. Also, we would like to thank the Varian Medical Systems and Elekta oncology systems for providing us with the specifications needed for the Linac treatment head simulations.

REFERENCES

1. Mackie TR and Battista JJ (1984) A macroscopic Monte Carlo method for electron beam dose calculations: a proposal, In: the use of computers in radiation therapy. Proceedings of the eight ICCR, Toronto, Canada.
2. Sheikh-Bagheri D and Rogers DWO (2002) Sensitivity of megavoltage photon beam Monte Carlo simulations to electron beam and other parameters. *Med Phys,* ***29****: 379-390.*
3. Sheikh-Bagheri D and Rogers DWO (2002) Monte Carlo calculation of nine megavoltage photon beam spectra using the BEAM code. *Med Phys,* ***29****: 391-402.*
4. Verhaegen F and Seuntjens J (2003) Monte Carlo modeling of external radiotherapy photon beams. *Phys Med Biol,* ***48****: R107-R164.*
5. Mesbahi A, Allahverdi M, Gharaati H (2005) Monte Carlo dose calculations in conventional thorax fields for Co60 photons. *Radiat Med,* ***23****: 341-350.*
6. Mesbahi A, Fix M, Allahverdi M, Grein E, Gharaati H (2005) Monte Carlo calculation of Varian 2300C/D linac photon beam characteristics: a comparison between MCNP4C and GEANT3 and measurements. *Appl Radiat Isot,* ***62****: 464-477.*
7. Mesbahi A, Reilly A, Thwaites D (2006) Development and commissioning of a Monte Carlo photon beam model for Varian Clinac 2100EX linear accelerator. *Appl Radiat Isot,* ***64****: 656-662.*
8. Mesbahi A, Reilly A, Thwaites D (2006) Experimental and Monte Carlo evaluation of Eclipse treatment planning system for lung dose calculations. *Rep Pract Oncol Radiother,* ***11****: 1-11.*
9. Farajollahi AR and Mesbahi A (2006) Monte Carlo dose Calculations for a 6 MV photon beam ina thorax phantom. *Radiat Med,* ***24****: 269-276.*
10. Mesbahi A (2006) Development a simple point source model for Elekta SL-25 linear accelerator using MCNP4C Monte Carlo code. *Iran J Radiat Res,* ***4****: 7-14.*
11. Faddegon BA , Ross CA, Rogers DWO (1991) Angular distribution of bremsstrahlung from 15-MeV electrons incident on thick targets of Be, Al and Pb. *Med Phys,* ***18****: 1727-39.*
12. Faddegon B, Egley B, Steinberg T (2004) Comparison of beam characteristics of a gold x-ray target and a tungsten replacement target. *Med Phys,* ***31****: 91-7.*
13. Butson MJ, Cheung T, Yu P, Carolan M, Metcalfe PE (2000) Simulation and measurement of air generated electron contamination in radiotherapy. *Radiation Measurements,* ***32****: 105-111.*
14. Malataras G, Kappas C, Lovelock DMJ (2001) A Monte Carlo approach to electron contamination resources in the Saturne-25 and -41. *Phys Med Biol,* ***46****: 2435-2446.*
15. Medina AL, Teijeiro A, Garcia J, Esperon J (2005) Characterization of electron contamination in megavoltage photon beams. *Med Phys,* ***32****: 1281-1291.*
16. Yang J, Li J S, Qin L, Xiong W, Ma C-M (2004) Modelling of electron contamination in clinical photon beams for Monte Carlo dose calculation. *Phys Med Biol,* ***49****: 2657-2673.*
17. Briesmeister JF (2000) MCNP-a general Monte Carlo N-particle transport code, Version 4C. Report LA-13709-M, Los Alamos National Laboratory, NM.
18. Podgorsak EB, Rawlinson JA, Glavinovic MI, Johns HE (1974) Design of X-ray targets for high energy linear accelerators in radiotherapy. *Am J Roentgenol Radium Ther Nucl Med,* ***121****: 873-82.*
19. Vassiliev ON, Titt U, Kry SF, Poenisch F, Gillin M, Mohan R (2006a) Monte Carlo study of photon fields from a flattening filter-free clinical accelerator. *Med Phys,* ***33****: 820-827.*
20. Vassiliev ON, Titt U, Kry SF, Poenisch F, Gillin M, Mohan R (2006) Dosimetric properties of photon beams from a flattening filter free clinical accelerator. *Phys Med Biol,* ***51****: 1907-1917.*
21. Pearson D, Parsai E, Fledmeier J (2006) Evaluation of dosimetric properties of 6 & 10 MV photon beams from a linear accelerator with no flattening filter. *Med Phys,* ***33****: 2099.*
22. Ding GX (2002) Energy spectra, angular spread, fluence profile and dose distribution of 6 and 18 MV photon beams: results of Monte Carlo simulations for a Varian 2100EX accelerator. *Phys Med Biol,* ***47****: 1025-46.*
23. Paelinck L, De Wagter C, Van Esch A, Duthoy W, Depuydt T, De Neve W (2005) Comparison of build-up dose between Elekta and Varian linear accelerators for high-energy photon beams using radiochromic film and clinical implications for IMRT head and neck treatments. *Phys Med Biol,* ***50****: 413-28.*